Available online at www.sciencedirect.com
SCIENCE DIRECT®
Journal of Power Sources 147 (2005) 288–294
JOURNAL OF POWER SOURCES
www.elsevier.com/locate/jpowsour

The parallel combination of a VRLA cell and supercapacitor for use as a hybrid vehicle peak power buffer

Paul Bentley [a,*], David A. Stone [a], Nigel Schofield [b]

[a] *The University of Sheffield, Department of Electronic and Electrical Engineering, Mappin Street, Sheffield S1 3JD, UK*
[b] *The University of Manchester, Institute of Science and Technology, UK*

Received 13 September 2004; received in revised form 15 January 2005; accepted 17 January 2005
Available online 2 March 2005

Abstract

The performance of a standard, production VRLA cell has been improved by paralleling with combinations of supercapacitors. The supercapacitors act to lower the source impedance of the combination providing a much-enhanced performance. Transient voltage swings are suppressed and the rms voltage is supported. Low-temperature performance may also be improved due to the characteristics of the supercapacitor. These enhancements are described for various combinations of cell and supercapacitor under realistic hybrid vehicle power demands. A simple model is proposed and used to demonstrate supercapacitor size requirements for optimal current in the parallel cell.
© 2005 Elsevier B.V. All rights reserved.

Keywords: Lead acid; Supercapacitor; Hybrid electric vehicles; Automotive; Batteries

1. Introduction

Recent increased interest in hybrid vehicles has been primarily motivated by the perceived improvement in fuel efficiency obtained with these vehicle topologies, when compared to similar all ICE based vehicles. However, currently only a handful of hybrid electric vehicles (HEV) are offered for sale on the forecourt, as whilst the adoption of hybrid drive systems leads to gains in fuel efficiency, lowering of vehicle emissions and improvements in vehicle performance, the high costs of state-of-the-art battery technologies such as NiMH and LiIon, used as peak power buffers in these vehicles, is considerable. Currently, the use of cheaper modern valve regulated lead acid (VRLA) cells within a hybrid-electric vehicle is prohibitive, due to considerably reduced cell lifetime experienced under the partial state-of-charge (PSoC) cycling, normally encountered within a hybrid vehicle.

Hybrid driving demands are characterised by high power discharge and charge pulses that occur during vehicle acceleration and regenerative braking, respectively. These pulsed currents reduce overall VRLA cell runtime, and overall battery health, by two mechanisms [1,2]:

1. Physical degradation of the cell structure. Pulsed currents normally encountered by the battery lead to higher rms cell currents, with accompanying higher operating temperatures. This gives rise to considerably shorter cell lifetime, due to increased grid corrosion, and increased gassing within the cell, leading to separator dry out, and eventual cell failure.
2. Higher currents lead to reduced available capacity. This reduced capacity is caused by the isolation of active material due to the blocking of pores by sulphate deposition during high rate discharge. Also the reaction rate may outstrip the diffusion rate causing a depletion of ions at the reaction surface [3].

In addition, high current pulses will create short duration low-cell voltages due to the Ohmic voltage drop caused by the cell's internal resistance. These low-voltage pulses in-

* Corresponding author. Tel.: +44 114 2225566.
E-mail address: elp98pb@sheffield.ac.uk (P. Bentley).

0378-7753/$ – see front matter © 2005 Elsevier B.V. All rights reserved.
doi:10.1016/j.jpowsour.2005.01.016

turn may trip low-voltage limit detection systems in closely managed battery packs.

As an example, the road data collected from a Honda Insight hybrid vehicle shows peak charge and discharge currents of approximately 50 and 90 A, respectively into the standard NiMH battery pack supplied with the vehicle, when subjected to a series of vehicle driving tests [4]. Small commercially available VRLA cells tend not to have the current capability required of a hybrid power system's peak power buffer, as the terminals of a typical spiral wound VRLA, of comparable ampere-hour (Ah) capacity to that of the NiMH cell used within the Insight's battery pack, are only designed to accept a 16 A push fit spade terminal. Therefore, whilst the VRLA cell would be able to supply the required energy, its power capability would be seriously reduced when compared to that of the NiMH cell.

A number of hybrid vehicle system have been proposed with the use of supercapacitors as the peak power buffer [5–7], however whilst the power capability of supercapacitors is adequate for HEV use, their energy storage capacity may not be great enough. For example, a Maxwell 2500 F supercapacitor stores only $\frac{1}{17}$th of the energy of the aforementioned VRLA cell. This is due to the steep slope of the capacitors voltage versus charge characteristic. However, supercapacitors do have a very repeatable high power capability and a significantly long lifetime when compared to most standard electrochemical cells. A parallel combination of supercapacitor and VRLA cell will therefore form a novel peak power buffer, whilst remaining an economically viable proposition. Under this operating scenario, the cell supports the bulk energy requirements of the vehicle, whilst the supercapacitor supports the majority of the peak-current output and sink requirements.

The idea of coupling supercapacitors and cells is not new. This approach has been made for lower power applications such as laptop computer and mobile phone batteries, notably to support lithium ion cells [1]. Although Holland et al. showed in [2] that coupling a Li-ion cell and supercapacitor, and testing under a simple pulsed current load provided only a marginal increase in available capacity. Further, systems employing individual banks of both cells and supercapacitors have been applied to electric vehicles [8,9]. Under these conditions, vehicle range is improved together with battery lifetime, at the expense of the requirement for a high-current, dc to dc converter to efficiently manage the energy flow within the vehicle, imposed by the large voltage swings experienced by the supercapacitor bank. Also, active balancing circuits are necessarily employed within the strings of supercapacitors to limit voltage mismatches as serious device damage can occur if supercapacitor peak voltage ratings are exceeded [10]. However the voltage range of the VRLA cell (approximately 1.7–2.45 V at the 1 C rate) is well matched to that of supercapacitors (typical peak voltage rating of 2.8 V), allowing the direct parallel connection of the two devices.

It is well documented [11,12] that the overcharging of VRLA cells can lead to excessive gassing and venting, cells should therefore be well ventilated due to the explosive and corrosive properties of the gaseous mixture. The effective management of cell voltages will limit the occurrence of such venting and prolong cell lifetime. To accomplish this simple FET based bypass devices can be applied to cells, this approach is also used for active balancing circuits in supercapacitor banks. When VRLA cells are directly paralleled with supercapacitors, the closed oxygen cycle of a VRLA cell may act as a simple bypass device, which in-turn, lowers the required rating of any external balancing or bypass circuitry needed when operating such couples within a battery string.

2. Experimental investigation

To ensure the cells/supercapacitors were subject to typical HEV driving cycles, real battery pack data was collected from a Honda Insight driven on the Millbrook test track [4]. The driving cycle included sections of urban stop-start driving, aggressive driving on the hill circuit and motorway driving with speeds up to 150 kph. Battery current and voltage data logged during driving was then used to create a 'typical' power demand profile of 2400 s duration, this then being scaled to represent the power demand that is experienced by one VRLA cell within a pack. An example of this power profile, scaled for a single cell, is illustrated below in Fig. 1. Positive power indicates cell charging, whilst negative power indicates cell discharge. This 'standard' profile was then applied to a number of cell/supercapacitor combinations to ascertain their performance under typical HEV driving conditions, the cells used in the tests being Hawker Cyclon 8 Ah (at the 5 h discharge rate) VRLA cells of a nominal capacity similar to that of the NiMH cells used in the Honda Insight hybrid vehicle (6 Ah 1 h discharge rate), together with supercapacitors manufactured by both EPCOS and Maxwell.

The driving cycles were applied to the cell/supercapacitor combinations in a purpose built high power cell test bench, constructed to allow the continuous testing of cells and supercapacitors under the applied test profile, and controlled ambient temperature. The test bench consists of a computer controlled bidirectional power supply, shown schematically in Fig. 2, allowing controlled currents of up to ±100 A. The control loop allows a demand bandwidth of 100 Hz, and data

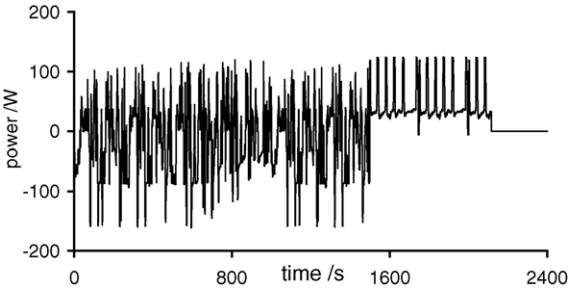

Fig. 1. Test power profile for one VRLA cell.

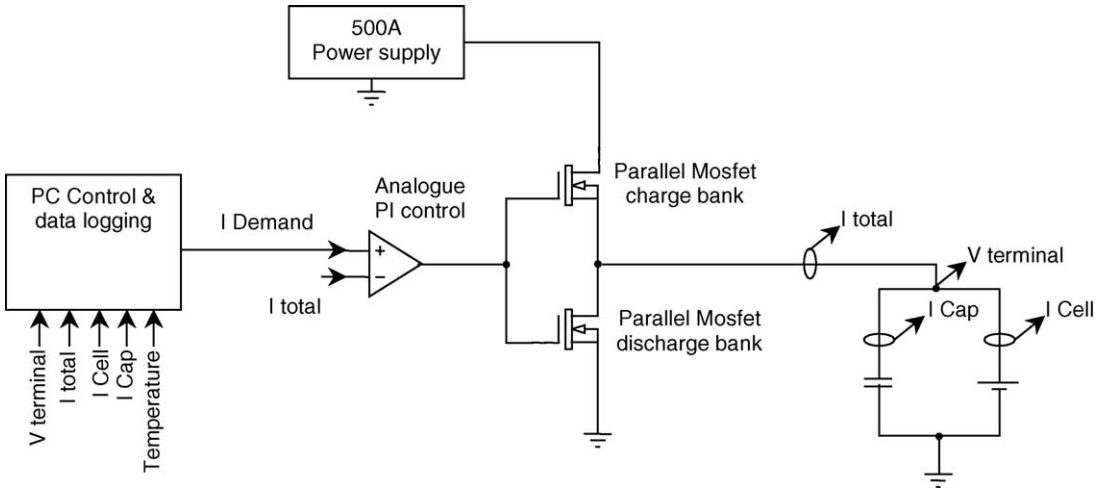

Fig. 2. Power cycler schematic.

collection occurs at up to 1 kHz. The measurement resolutions are 0.3 mV and 3 mA for cell voltage and current, respectively.

As the test profile utilised is a power profile, the instantaneous cell current demand is dependant on the actual cell voltage at any point during the test. Under these conditions, if the cell voltage drops rapidly due to the cell approaching 0% SoC, the current demand on the cell increases, leading to a positive feedback mechanism and subsequent end of the test when it reaches the 100 A cell maximum current demand set within the system, this limit being imposed to mimic the 100 A maximum current limit observed on the actual vehicle.

As cells are ideally held in a partial state-of-charge under standard hybrid operation, to allow ample available capacity for power assist, whilst retaining the ability to efficiently absorb charge during regenerative braking [13], an initial cell SoC of 80% of the cells known 5 h charge capacity was chosen for this investigation. Prior to testing, the cells were conditioned to bring them to full capacity, following the manufacturers recommended conditioning routine. This routine involved four cycles of full charge and discharge of the cells, the charging being over 16 h at a constant cell voltage of 2.45 V, with a 10 A current limit, in a controlled ambient temperature of 25 °C. The following discharge was then carried out at a constant current of 1.53 A, to a low-voltage cut-off point of 1.70 V, once again within a controlled ambient temperature environment of 25 °C. After conditioning, the cells were then discharged from an initial 100% SoC, to the test start-point of 80% SoC, with a 1.53 A discharge, prior to the power cycling. To minimise transient currents when connecting the supercapacitors in parallel with the cells under test, the supercapacitors were initially charged to the open circuit voltage of the cells prior to the connection being made. The parallel arrangement of cell and supercapacitor was then 'soaked' in an ambient temperature of 40 °C prior to the tests, this temperature being chosen, as it is close to the optimum operating temperature for VRLA cells under standard hybrid duty [14,15].

3. Observations and discussion

Initially, cycling of a single Cyclon cell to provide reference data, showed that the cell on its own was incapable of completing the full power profile. The unassisted cell failed to complete the full test due to a current demand of more than the permitted maximum of 100 A, during a discharge pulse, after just over half the test cycle (1300 s). The current limit for these tests is set to match that of the Honda Insight's system, as discussed earlier.

The addition of a single 100 F supercapacitor in parallel with the cell improved the overall performance slightly, extending the run-time of the test to 1400 s, however, the addition of the 1250 and 2500 F capacitors dramatically improved the overall performance, reducing the cell/supercapacitor voltage excursions, and allowing the cell/capacitor combination to complete the driving cycle, as the addition of the larger capacitors reduced the overall current demands placed on the cell as compared with the unassisted cell. As the increasing capacitance improved the voltage regulation of the parallel cell/capacitor combination, the total current demand on the pair also decreased as a consequence of the power demand profile used in the tests. The lower internal impedance of the larger supercapacitors, when compared with that of the cell lead to the larger supercapacitors supplying/sinking a large fraction of the transient currents demanded by the test system, the total voltage equalising the charge after the transient. This is clearly illustrated in Figs. 3–6, which show the current division between the cell and a 2500 F capacitor in parallel, and illustrate the nature of the loading on the pair during hybrid power cycling.

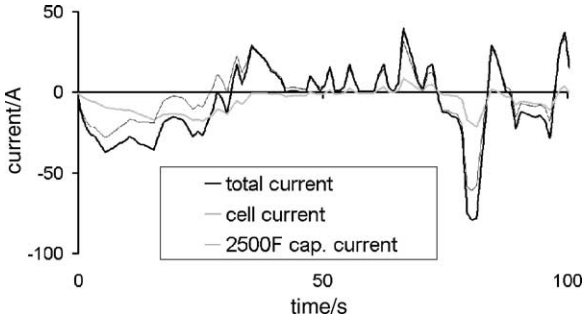

Fig. 3. Section of current profiles during power cycling.

Fig. 3 illustrates the division of current between the cell and 2500 F supercapacitor at the start of the power profile. Here it can be seen that the short time constant of the supercapacitor allows it to both supply and sink the bulk of the demanded current pulses, applied to the cell/capacitor pair, whilst the magnitude of the cell current remains low. During instances when the cell/capacitor pair has been discharging for a few 10 s of seconds, the cell takes over the supply of the bulk current, as during the first 30 s of Fig. 3. This effect is also seen during the first 20 s of Fig. 4. The cell current then remains negative as the total current and supercapacitor current both become positive. The cell is effectively recharging the supercapacitor during this period.

During the last section of the power profile the cell/capacitor pair was returned to 80% SoC by the application of regenerative 'braking' pulses. This is illustrated in Fig. 5. Here it can be seen that the supercapacitor absorbed the bulk of the dynamic regenerative current at each pulse. Between the pulses, the supercapacitor is effectively charging the cell. Thus the cell, which is the bulk energy store of the pair, was steadily recharged during this period.

At the end of the power cycle it can be seen, from Fig. 6, that the supercapacitor continued to charge the cell whilst the total current from the cell/capacitor pair was zero. This corresponds to the relaxation of the cell and supercapacitor over potentials, as an equilibrium state was approached.

The rms and maximum currents for each cell and supercapacitor pair are shown in Table 1 and illustrated in Fig. 7. These comparisons cover the period up to 1300 s of the cycle, which the unassisted cell completed successfully, and allows a true comparison of all the combinations examined. A simple quadratic fit was found to produce a good match to the curve in Fig. 7. The rms current is responsible for the majority of the heating effects in the cell, through Ohmic

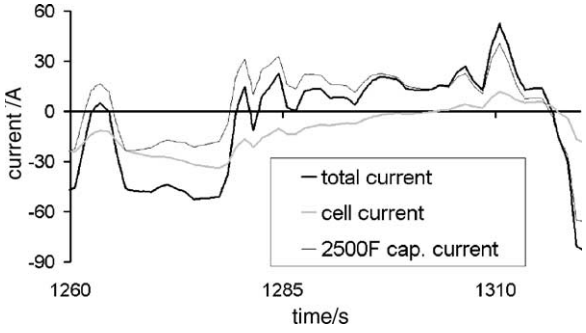

Fig. 4. Cell charging super capacitor during power cycling.

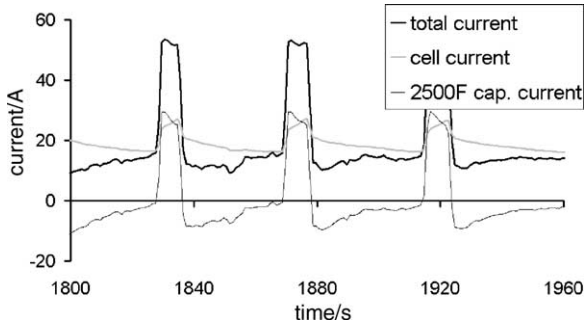

Fig. 5. Capacitor charging cell during regeneration pulses.

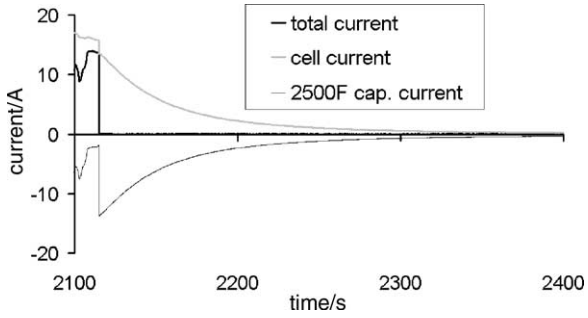

Fig. 6. Capacitor charging cell at end of power cycle.

Table 1
Comparison of rms cell current during cycle

Combination	Rms cell current (A)	Maximum cell current (A)
Cell alone	25.91	100 (maximum allowed for insight system)
Cell and 100 F supercapacitor	23.39	93.848
Cell and 1250 F supercapacitor	13.17	49.1959
Cell and 2500 F supercapacitor	10.81	37.744

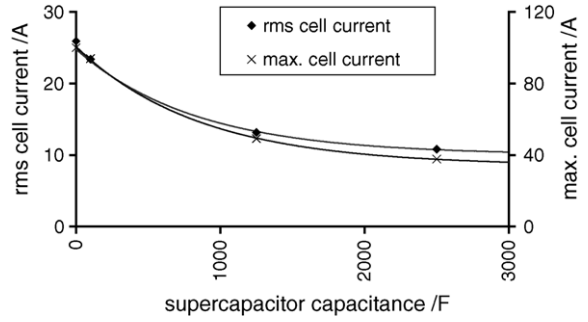

Fig. 7. Relationship between rms and maximum cell currents to supercapacitor size.

Table 2
Comparison of NiMH pack cell weight and volume to that of the proposed replacement 2supercapacitor/VRLA cell based pack

	144 NiMH cells	72 VRLA cells	72 Supercapacitors	Cell/supercapacitor pack
Weight/kg	24.5	39.5	22.5	62
Volume/l	7.49	11.2	14.2	25.4

(I^2R) losses. Minimising this heating will have beneficial effects on cell lifetime, as gassing and hence electrolyte loss and also grid corrosion, are all temperature dependant. As the spade terminals of the cyclon cell are rated for a 16 A continuous current, and assuming that the internal resistance of the supercapacitors scales in proportion to their capacitance, then from the curve fits to Fig. 7, a supercapacitor of slightly less than 1250 F in parallel would limit the cell current to its terminal rating of 16 A rms. This value of supercapacitor also halves the maximum current imposed on the cell when compared with that imposed on the unassisted cell.

For sake of comparison, data taken from [10] was interpolated to estimate the weight and volume for a 1250 F supercapacitor. Hence, the weight and volume for a pack made up from cell/supercapacitor couples was calculated. Table 2 gives a comparison of the original Honda Insight NiMH cells' volume against that of the proposed replacement pack components and pack formed from supercapacitor and VRLA cells.

The table demonstrates that a weight penalty of approximately 2.5 times and volume penalty of approximately 3.4 times, would be imposed by the adoption of the proposed cell supercapacitor couple to replace the standard NiMH system.

4. Combined cell/supercapacitor model

One problem encountered with the modelling of state-of-charge (SoC) for Lead Acid cells, is the difficulty in predicting the cells charge acceptance behaviour under large regenerative pulsed currents [16]. The use of a parallel combination of cell and supercapacitor significantly reduces the current pulse seen by the cell, and hence lowers the cell overvoltages present on re-charge. Therefore a simple electrical model is proposed to predict the dynamic performance of the cell/supercapacitor parallel pair under realistic hybrid driving conditions, and enable SoC prediction for the cell. In this proposed model, the supercapacitor is modelled as a large ideal capacitance in series with a finite internal resistance. As the cell exhibits an almost linear voltage drop on a low-current constant rate discharge until almost fully discharged, the cell may also be approximated by a large ideal capacitance, once again in series with a finite internal resistance. The values for the effective capacitances of the cell and supercapacitors were obtained using the following procedure, and the model was initially implemented within the Spice electrical simulation package, as illustrated in Fig. 8, to enable model verification.

The values of the capacitors used to model both the cell and the supercapacitor were obtained by discharging both the cell, and the supercapacitor, separately at the cells nominal 5-h rate of 1.53 A, after initially being charged to the cells full SoC open circuit voltage. The discharge was terminated in both cases with a low-voltage limit of 1.7 V, representing 0% SoC for the cell. The effective capacitance of the devices can then be found from the relationship $C = \Delta Q/\Delta V$, and are listed in Table 3.

As expected, the calculated capacitances of the supercapacitors were similar to the expected 'name-plate' values, the

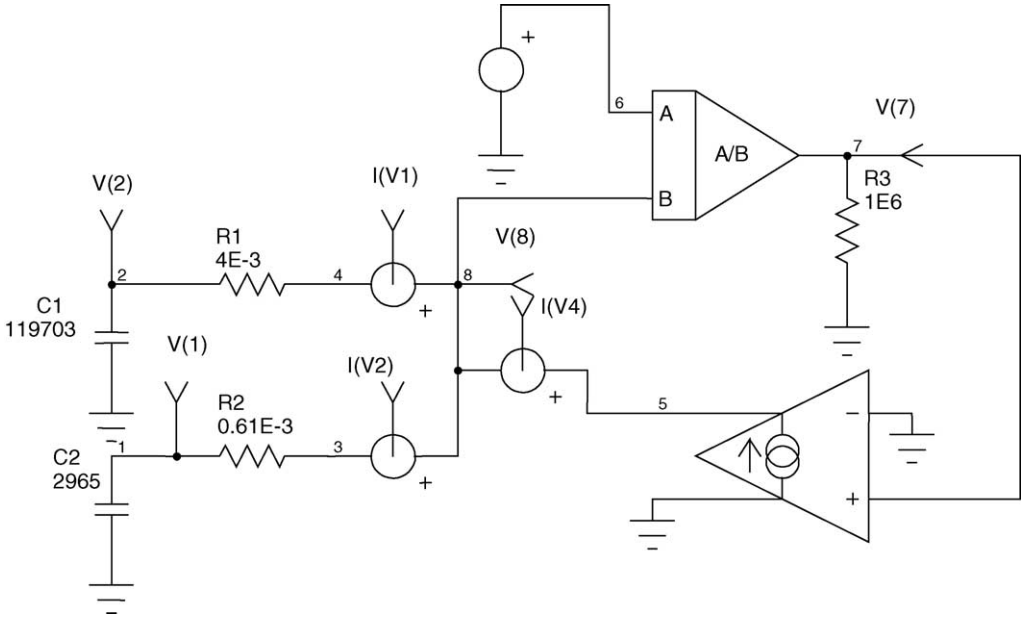

Fig. 8. Spice model to simulate capacitor and cell on power profile.

Table 3
Calculated capacitances for capacitors and cell

Device	Calculated capacitance (F)
EPCOS 100 F	104
Two MAXWELL 2500 F in series (1250 F)	1,267
MAXWELL 2500 F	2,965
Cyclon VRLA cell	119,703

capacitance of the cell exceeding the largest supercapacitor by a factor of 40. The charge capacity of the Maxwell 2500 F capacitor was found to be 0.405 Ah, $\frac{1}{17}$th of that of the VRLA cell, and the energy removed during the voltage excursion of the test was 2.838 kJ. Similarly the 100 F capacitor had significantly smaller charge capacity of 0.008 Ah, and energy capacity of 0.054 kJ.

To calculate the internal resistance of both the cell and supercapacitors, they were discharged individually at 40 °C using a 12 A constant current. At 500 s intervals during the discharge a 1 Hz 5 A amplitude 5 A offset discharge (0–10 A peak discharge) excitation was applied for 10 s. The voltage and current response to the excitation was then used to find the internal resistance of the cell and capacitor. The overall slope of the constant current discharge was also used to calculate the capacitance of the cell and capacitor. The mean cell internal resistance for each set of pulses was as shown in Fig. 9.

The mean capacitor internal resistance was calculated to be 0.61 mΩ and the mean cell internal resistance was calculated to be 4.17 mΩ. When used in the model, the above values gave a mean error in the terminal voltage of 0.0094 V as illustrated by the percentage error in terminal voltage between the actual measured value and the simulated value, shown in Fig. 10. The highest error between the actual and simulated terminal voltage occurs during the high recharge portion of the power profile, when the highest polarisations voltages will occur within the cell. Whilst the model proposed is extremely simple, and easy to implement within a battery management system (BMS), the model fails to take into account the activation and concentration over potentials. Miller suggests that the simple capacitor and internal resistor model is too simplistic and proposes a more complex capacitor and resistor ladder network [17]. However, more complex models

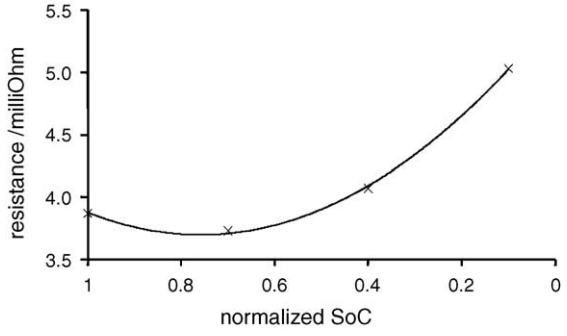

Fig. 9. Variation of cell internal resistance with normalised SoC.

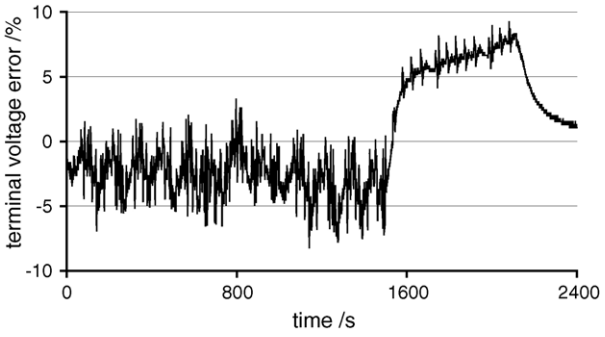

Fig. 10. Percentage voltage error between simulation and experiment.

are currently under investigation with cell internal resistance and open circuit voltage made a function of SoC, in which a lumped parameters approach is being made to the representation of the activation and concentration over potentials of the cell.

5. Conclusion

In this paper we have proposed a VRLA cell/supercapacitor parallel combination as an effective HEV peak power buffer, in which the cell current drawn is reduced as the supercapacitor sources and sinks the majority of transient current. In turn, the cell as the bulk energy store, supports the relatively low-energy storage of the supercapacitor. The nature of power demands from urban driving provide ample periods for charge to be passed from cell to capacitor and vice versa, the exchange being governed by relative internal impedances and past discharge histories of the two power sources. A simple model was presented which allowed the optimum size of the supercapacitor to be been inferred from the results, and a basic measurement of SoC to be made. This approach therefore leads to the use of components that naturally complement each other's performance. The size and complexity of balancing circuits commonly applied to series strings of supercapacitors would be reduced in this application due to the closed oxygen cycle of the VRLA cell acting as an in built bypass circuit for the supercapacitor.

References

[1] T.A. Smith, J.P. Mars, G.A. Turner, Using supercapacitors to improve battery performance, in: Proceedings of the 33rd Annual IEEE Power Electronics Specialist Conference, vol. 1, 2002, pp. 124–128.
[2] C.E. Holland, J.W. Weidner, R.A. Dougal, R.E. White, Experimental characterization of hybrid power systems under pulse current loads, J. Power Sources 109 (2002) 32–37.
[3] H. Bode, Lead-Acid Batteries, Wiley, 1977, ISBN 0-471-08455-7, pp. 285–294.
[4] M.J. Kellaway, P. Jennings, D. Stone, E. Crowe, A. Cooper, Early results from a systems approach to improving the performance and lifetime of lead acid batteries, J. Power Sources 116 (2003) 110–117.

[5] D. Yang Jung, Y.H. Kim, S.W. Kim, S.-H. Lee, Development of ultracapacitor modules for 42-V automotive electrical systems, J. Power Sources 114 (2003) 366–373.
[6] A. Burke, M. Miller, Comparison of ultacapacitors and advanced batteries for pulse power in vehicle applications: performance life, and cost, in: Proceedings of the 19th Electric Vehicle Symposium, 2002, pp. 855–866.
[7] J. Folchert, D. Naunin, D. Tseronis, Ultra capacitor storages for automotive applications, in: Proceedings of the 19th Electric Vehicle Symposium, 2002, pp. 867–875.
[8] F. Gagliardi, M. Pagano, Experimental results of on-board battery-ultracapacitor system for electric vehicle applications, in: Proceedings of the IEEE, International Symposium on Industrial Electronics, 2002.
[9] P.H. Mellor, N. Schofield, D. Howe, Assessment of supercapacitor/flywheel and battery EV traction systems, in: Proceedings of the 33rd International Symposium on Automotive Technology and Automation, 2000, paper 00ELE044.
[10] A. Schneuwly, M. Bartshi, V. Hermann, G. Sartorelli, R. Gallay, R. Koetz, BOOSTCAP double-layer capacitors for peak power automotive applications, in: Proceedings of the AABC-2002, 2002.
[11] P. Reasbeck, J.G. Smith, Batteries for Automotive, Wiley Research Studies Press, 1997, ISBN 0863801765.
[12] D.A.J. Rand, R. Woods, R.M. Dell, Batteries for Electric Vehicles, Wiley Research Studies Press, 1998, ISBN 0863802052.
[13] F. Robert, Nelson, Power requirements for batteries in hybrid electric vehicles, J. Power Sources 91 (2000) 2–26.
[14] A.A. Pesaran, D. Swan, J. Olson, J.T. Guerin, S. Burch, R. Rehn, G.D. Skellenger, Thermal analysis and performance of a battery pack for a hybrid electric vehicle, in: Proceedings of the Electric Vehicle Symposium EVS 15, Brussels, Belgium, 1998.
[15] Ahmad A. Pesaran, M. Keyser, Thermal characteristics of selected EV and HEV batteries, in: Proceedings of the IEEE, The 16th Annual Battery Conference on Applications and Advances, 2001, pp. 219–225.
[16] S. Piller, M. Perrin, A. Jossen, Methods for state-of-charge determination and their application, J. Power Sources 96 (2001) 113–120.
[17] J.R. Miller, Development of equivalent circuit models for batteries and electrochemical capacitors, in: Proceedings of the IEEE, The 14th Annual Battery Conference on Applications and Advances, 1999, pp. 107–109.